Ground motion simulation for earthquakes in Sumatran region

J. Dhanya and S. T. G. Raghukanth*

Department of Civil Engineering, Indian Institute of Technology Madras, Chennai 600 036, India

The present study aims at developing a model for simulating ground motion for earthquakes in the Sumatran region where one of the most devastating earthquakes took place in 2004 with a moment magnitude (M_w) of 9.1. With advancements in instrumentation, the three-dimensional material properties, topography and bathymetry of the region are available in the global database. These parameters are used as inputs in Spectral Finite Element Method to simulate ground motions. The model is first validated with the IGCAR broadband velocity data for 2012 M_w 8.6 Sumatra Earthquake. Due to favourable comparison, our model is also used to generate ground displacement characteristics of M_w 9.1 event. The source uncertainties are accounted by using three finite fault slip models available in the global database. The simulated time histories showed that the ground motion is sensitive to input slip models. The peak ground displacement (PGD) and ground residual displacement (GRD) in both horizontal and vertical directions are presented as contour plots. PGD obtained from various slip models in the epicentral region is of the order of 14–22 m in horizontal direction and 7–16 m in vertical direction. GRD in the epicentral region is of the order of 6–17 m in East–West (E–W) 4–17 m in the North–South (N–S) directions. The vertical uplift obtained from various slip models is around 2–8 m. The developed model can be used to simulate ground motion time histories, which can be further used in hazard analysis, tsunami simulations, etc.

Keywords: Ground motion time history, ground residual displacement, peak ground displacement, Sunda arc.

GROUND motion characteristics of an earthquake are essential to understand the hazards posed by the event. The near-field features of ground motion could be understood better if an array of strong motion network is present in the region. In the absence of such recorded data, one has to resort to analytical, numerical and/or empirical techniques to estimate the synthetic data of the ground motions. In the present study, a model has been developed to simulate ground motions for earthquakes in the Sumatran region. This study is of particular importance in this region, as it possesses very high seismicity due to the active subduction of the Indo-Australian plate beneath the Burma Plate. Based on earthquake recurrence parameters, Pailoplee and Choowong[1] showed the potential for a large thrust earthquake in the region. Further, based on Global Positioning System (GPS) measurements, Ortiz and Bilham[2] have reported that the return period for the great earthquake in region could be 114–200 years. One of the great earthquakes that occurred in the recent past in the region is the devastating (M_w 9.1) 2004 Sumatra earthquake. This earthquake and the subsequent tsunami led to a heavy loss to both life and property. According to the report of Asian Disaster Preparedness Center (ADPC), the event affected 10 countries causing a global death toll of 0.22 million people. The event also led to a major economic loss of US$ 9.9 billion in Asia. The estimated cost of reconstruction amounted to at least US$ 7.5 billion. Following this earthquake, many researchers have worked on various aspects like the rupture process[3–5], modelling tsunami wave characteristics[6–8], deterministic hazards and vulnerability assessment due to the tsunami generated from the region[9,10], etc. With regard to ground motion simulation, Sørensen[11] employed a hybrid method to simulate peak ground acceleration and peak ground velocity contours. However, the use of one-dimensional velocity model to represent medium and single earthquake source characteristics considered for the particular study raises concern regarding the reliability of the estimated ground motion data. Further, for modelling of the tsunami waves, the ground displacements are the essential boundary conditions. In general, the tsunami simulation for this event is performed based on static displacements[12] estimated from analytical methods, e.g. Okada[13]. These analytical techniques which consider the medium as elastic half space do not account for material nonlinearity and sphericity of the earth. In addition, it should be noted that the dynamic characteristics of the ground displacement time histories should also be considered for the simulation of tsunami waves[14].

It is known that great earthquakes rupture large areas of a region (2004 Sumatra earthquake ruptured ~1100 km of fault length). Hence, one has to resort to a numerical technique that can handle geometrical complexities like topography, bathymetry and sphericity of the earth better than methods based on layered elastic half space. With numerous advancements in the simulation techniques, it is still a challenge to develop realistic ground motions

*For correspondence. (e-mail: raghukanth@iitm.ac.in)

due to the uncertainties in source and medium characteristics of the region. Hence it is a common practice to validate ground motions generated for an event using the model developed with data available in seismic networks for that event. One such network in India is at the Indira Gandhi Centre for Atomic Research (IGCAR), Kalpakkam, which got commissioned in 2008. Thus it would be relevant to develop a model to simulate ground motion for the region, that is validated with data available in the IGCAR network.

In this article, the possible ground displacement time histories are simulated using spectral finite element method (SPECFEM). The SPECFEM models were earlier developed for Gujarat[15], Delhi[16], Nepal[17] and other regions. A similar method is adapted to model the South Asian region to simulate displacement time histories for earthquakes in the region. The developed model is validated with data available from the IGCAR database for the great (M_w 8.6) 2012 Sumatra earthquake. In view of the favourable comparison, the model can be further used to simulate ground motions for the region. The model is further employed to determine the ground motion characteristics of the 2004 Sumatra earthquake for various slip distributions available in the global database. The ground motions in the epicentral region for this event are represented in terms of peak ground displacement (PGD) and ground residual displacement (GRD) contour maps, which are respectively the contours of maximum and final value of time histories simulated at various stations on a grid in the region. The sensitivity of the source model is analysed by comparing the ground motion time histories for near source stations like Port Blair, Neil Island, and Nicobar Island and for distant source stations like Chennai, Vizag, Pondicherry, Kanyakumari, etc.

Tectonic settings

The tectonic setting in the northeastern part of the Indian Ocean is complex compared to other regions of India. Seismicity along with fault lines identified in the region is shown in Figure 1. This region is a subduction-zone with Indo-Australian Plate submerging into the Eurasian Plate. This subduction resulted in the formation of a deep trench, a back-arc island and basins and a spreading centre (Andaman Sea Ridge (ASR))[18]. Several thrust and strike–slip faults are developed in the region due to this particular tectonic setting. Further, the Andaman-Sumatra region comes under the zone of high seismic hazard (Zone V) according to IS 1893: 2002 (ref. 19). The slip rate in the Sumatran fault system is about 11–28 mm/year (ref. 20). Based on GPS measurements, the convergence rate at certain parts of the Sunda arc region ranges to a maximum of 6–6.5 cm/year (ref. 21). This convergence rate decreases northwards as the azimuth of the trench becomes almost parallel to the direction of movement of the Indian Plate, thus resulting in strike–slip faults. In the historic and recent past, the region experienced several earthquakes of moderate-to-large magnitude[22]. In the last 250 years, there were around seven great earthquakes ($M_w > 8$) in the region. These are the earthquakes in 1797 ($M_w = 8.7$) rupturing 370 km of the fault, 1833 ($M_w = 9$) rupturing 500 km of the fault, 1861 ($M_w = 8.5$) rupturing 270 km beneath Nias Island, 2004 ($M_w = 9.1$), 2005 ($M_w = 8.6$), 2007 ($M_w = 8.4$) and 2012 ($M_w = 8.6$). Other than the 2004 Sumatra earthquake ($M_w = 9.1$), many thrust earthquakes as those in 1847, 1881 ($M_w = 7.9$) and 1941 ($M_w = 7.7$) were large enough to cause tsunami-like waves in the Indian Ocean[23]. The recurrence parameter calculation with respect to fractal dimension in the region shows the potential for a large thrust earthquake in the region[1].

Ground motion database

The data from seismic networks can be used to interpret the regional characteristics of an earthquake. In India, two such networks commissioned are the PESMOS, which mostly spread over the seismically active Himalayan belt and that present at IGCAR. In the present study, the data from IGCAR network is used as it is relatively nearer to the Sumatran region.

IGCAR network: In the IGCAR network, presently there are six stations including a central receiving station (CRS). The other five stations are Anupuram (ANP), Chengalpet (CPT), Illalur (ILL), Manamathi (MMT) and Palayam (PLM). Only the central station at IGCAR has a strong motion accelerometer whereas the others have broad band velocity seismometers. These stations have recorded ground motions of various earthquakes across the globe whose magnitude ranges from M_w 2 to M_w 9.1. The epicentres of these events along with the IGCAR broadband station locations are shown in Figure 2. Kavitha and Raghukanth[24] used 13 local event data from this network to develop and calibrate the stochastic seismological model. This is then used to formulate the ground motion prediction equation for the east coastal region of India. In the present study, the data available in the network for the 2012 (M_w 8.6) Sumatra earthquake is used for validation of the model. This being a great event in the Sumatran region, leads to better data-quality at the recording stations and hence could be used reliably for validation.

Methodology

The ground displacements in the near-field will be strongly influenced by the source and the medium characteristics. In the present study, ground displacement time histories are simulated using Spectral Element Method

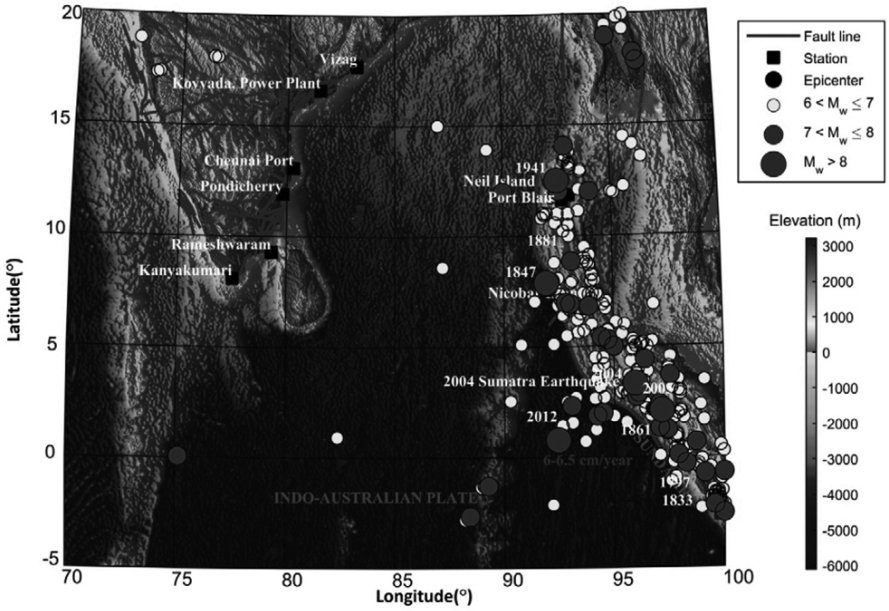

Figure 1. The tectonic setting of south Asian region (fault line as per GSI[31]).

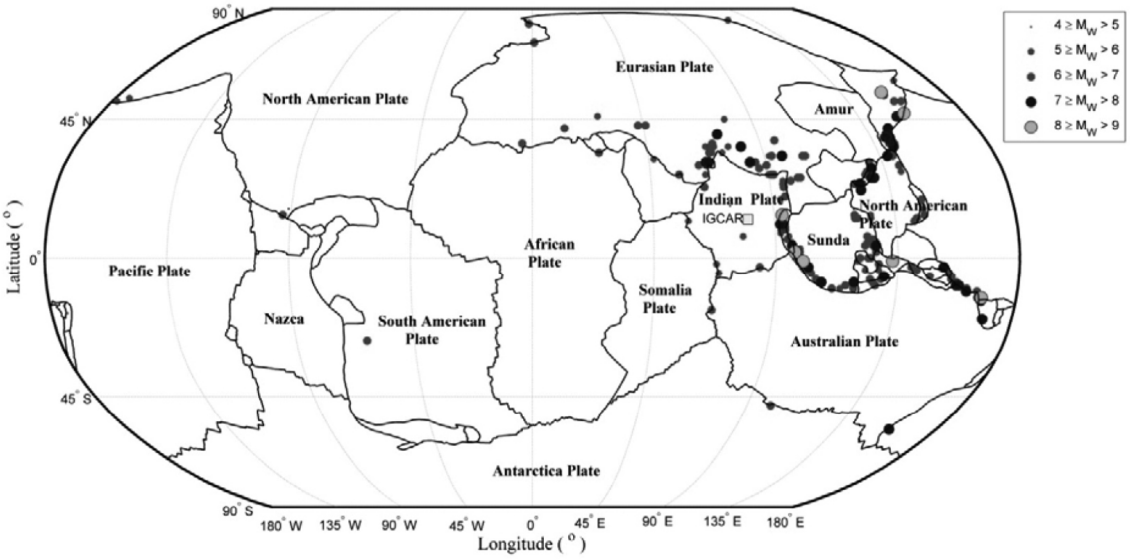

Figure 2. Teleseismic events recorded by IGCAR network.

(SEM). SEM was initially developed for computational fluid dynamics[25]. Later this method was applied for problems related to 2D and 3D seismic wave propagation[26], subsequently the method was extended to model the global seismic wave propagation[27,28]. One advantage of this method is the ease of implementation of free surface topography and lateral variation in material properties. It is also established that, given the input rupture details and medium properties, SPECFEM is capable of simulating near-field ground motion[17].

Here, the earth interior is broadly divided into crust, mantle, core and inner core. In the SPECFEM, the methodology governing equations is formulated for each of this region in the spherical domain according to the material characteristics of the region. Further, the boundary conditions like stress-free boundary at the surface and stress continuity at the interfaces of regions are imposed on the model. Then the weak form of the governing equation of each region is formulated by taking the dot product of the governing equation with an arbitrary vector w and imposing boundary conditions, which is the higher order variational method. In SPECFEM, as shown in Figure 3, the region considered is first discretized into non-overlapping hexahedral volume elements. Then, using

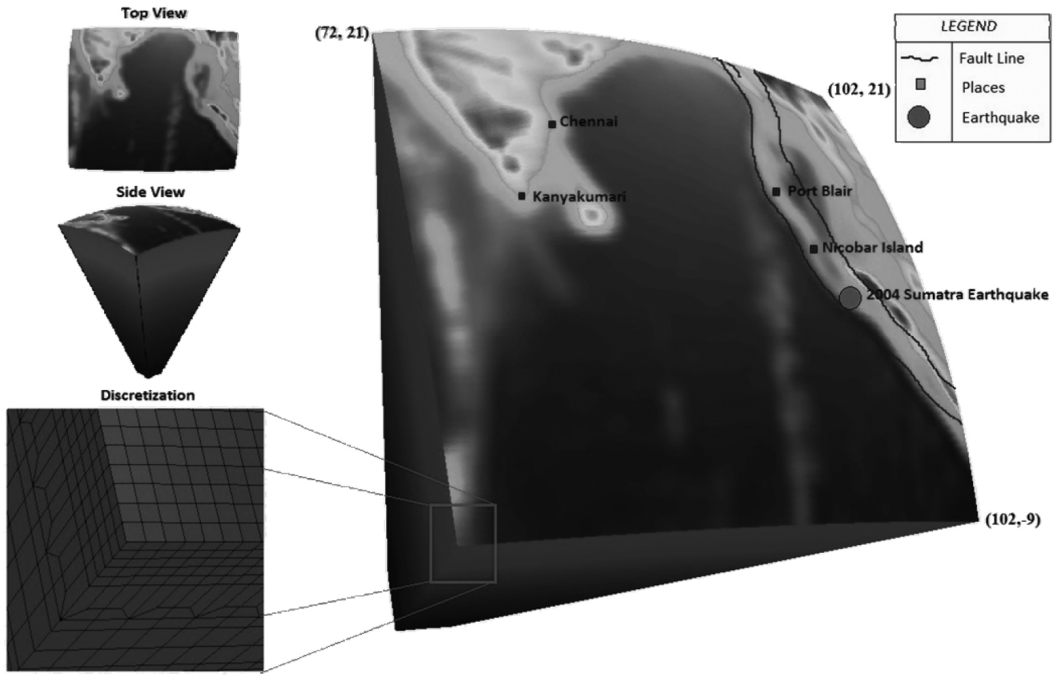

Figure 3. The SPECFEM chunk considered for the simulations along with the top view, the side view and the discretization of the chunk. (Note that the colour in the figure indicates the variation in topography.)

classical Jacobian matrix, each element is mapped to a reference cube. Lagrange interpolants is assumed to represent the displacement field in each element. Unlike the traditional finite element method, high-degree Lagrange interpolant is used to represent the basic functions for displacement field on the element in SPECFEM. The control points needed to define polynomial of order n is $(n + 1)^3$, i.e. Gauss–Lobatto–Legendre (GLL) points for each element in the mesh. In the hexahedral volume element, all basic functions for displacement field u are interpolated by triple products of Lagrange polynomials of degree n at these GLL points. The numerical integration of volume elements is approximated using GLL quadrature integration rule. GLL quadrature is exact for polynomials up to a degree $(2n - 1)$. Once the discretization of all the three regions in the Earth's interior is completed, the global system of equations to be solved by assembling contributions from individual elements can be written as

$$M\ddot{u} + C\dot{u} + Ku + Bu = F -^{28}, \quad (1)$$

where u is the global displacement vector along the three global degrees of freedom, i.e. North–South, East–West and vertical directions, M and K are the global mass matrix and global stiffness matrix respectively, C contains terms related to angular rotation vector, B is related to the region boundary interactions and $-F$ is the source term. The M, K, C, B and F matrix formulated from the integration weak form solutions at the elemental level and then assemble it in the global level. In the presence of ocean layer, the mass matrix, M is replaced by $M + m$, where m is the load from ocean layer. The advantage of the variational method along with Lagrange polynomial in conjunction with GLL quadrature is that it renders mass matrix diagonal, thus reducing the computational cost. The explicit expressions for M, C, K, B and F matrices at the elemental level and further construction of these matrices at the global level are available in the literature[26–28]. An explicit second order Finite Difference (FD) method, in general, known as Newmark scheme, is used to march the eq. (1) in time. This FD scheme is only conditionally stable.

The ground displacement time histories for the given event can be performed using both 3D regional and global algorithms. In the present study, since the earthquake rupture length is high (~1700 km), global spectral element algorithm, which accounts for the spherical geometry of the earth is utilized. The SPECFEM 3D Globe package has a set of FORTRAN subroutines to simulate the three-dimensional wave propagation for an earthquake event. In this model, the effects due to lateral variations in p-wave velocity, s-wave velocity, thickness of the crust, density, ellipticity, topography and bathymetry are included. In the present study, the simulation was performed by implementing the package in IBM System × iDataPlex dx360 M4 highly optimized servers with 2X Intel E5-2670 8C 2.6 GHz processor. Parallel programing based on message-passing interface (MPI) was used for executing the simulations. The simulation can be

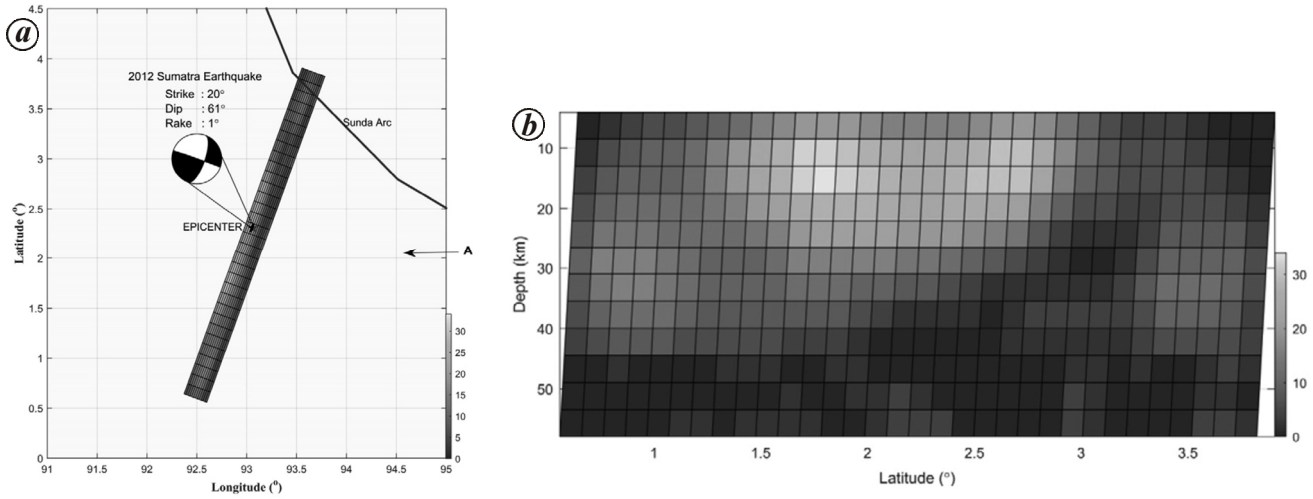

Figure 4. The slip distribution (in metre) of 2012 (M_w 8.6) Sumatra earthquake (reported by Wei[30]).

Table 1. Slip distribution characteristics for 2012 (M_w 8.6) Sumatra earthquake

Slip parameters	Wei[30]
Longitude, latitude	92.96, 2.267
Depth (km)	22
Length (km)	384
Number of segments	1
Hypocentre	
Along strike (km)	198
Down-dip (km)	22.5
Segment	
Length (km)	384
Width (km)	60
Strike (°)	20
Dip (°)	64
Average rake (°)	1
Number of sub-faults	384
Size of sub-faults (km)	12 × 5
Avg. rupture velocity (km/s)	2.6
Max. slip (m)	34

performed by mapping the entire globe onto a sphere divided into six chunks using 'cubed sphere' or using only one chunk covering the region under consideration. In this study, only one chunk covering the region as shown in Figure 3 was considered. For the medium, the 3D velocity model available for mantle and crust was used[29]. The 5-min topography and bathymetry (ETOPO5) from the global database (http://www.ngdc.noaa.gov/) was used to model the free surface topology. For the south Asian region, latitude 6°N and longitude 87°E is taken as the centre of the chunk. The chunk extends to an angular width of 30° × 30°. The surface other than the top of the chunk is provided with absorbing boundary conditions to avoid reflection of waves from these surfaces. The chunk is further subdivided into 16 slices in each direction on the surface. Each slice constitutes of 32 × 32 spectral element at its surface. Thus, the number of spectral elements in one chunk mesh is 13 million. Each spectral element consists of 125 grid points. Thus the entire chunk mesh is represented with a total of 872 million grid points with an average distance of ~4.88 km between grid points. The total number of degrees of freedom in the entire mesh is 2.4 billion. A total of 256 processors is used to handle the entire mesh considered for the region. It took approximately 30 min for the mesh generation. For source, the Centroid Moment Tensor (CMT) solutions for the slip models are used as finite source. The simulated displacements from the model are valid up to the shortest period of 14 sec. It requires almost 48 h to run the solver once.

Validation

The SPECFEM model considered for the region needs to be first validated with the recorded data. Thus, ground motions simulated using the SPECFEM model used in the present study is compared with recordings available at IGCAR network for 2012 Sumatra earthquake (M_w 8.6). The slip distribution for this event developed by Wei[30] is considered to represent the source in the model. This slip distribution is shown in Figure 4. Wei[30] derived this model by inversion of the Global Seismic Network (GSN) broadband data from IRIS-Data Management Center. This particular distribution is arrived at by analysing 31 teleseismic *P* waveforms selected based on data quality and azimuthal distribution[30]. The details of the slip distribution so obtained are summarized in Table 1. It can be noted that the rupture process for the particular event is mainly strike–slip with rake angle 1°. The rupture plane is discretized by subfaults of size 12 × 5 km on a surface of length 384 km along the strike angle (the angle that the fault plain makes with north direction) of 20° and width 60 km along the dip angle (the angle that the fault

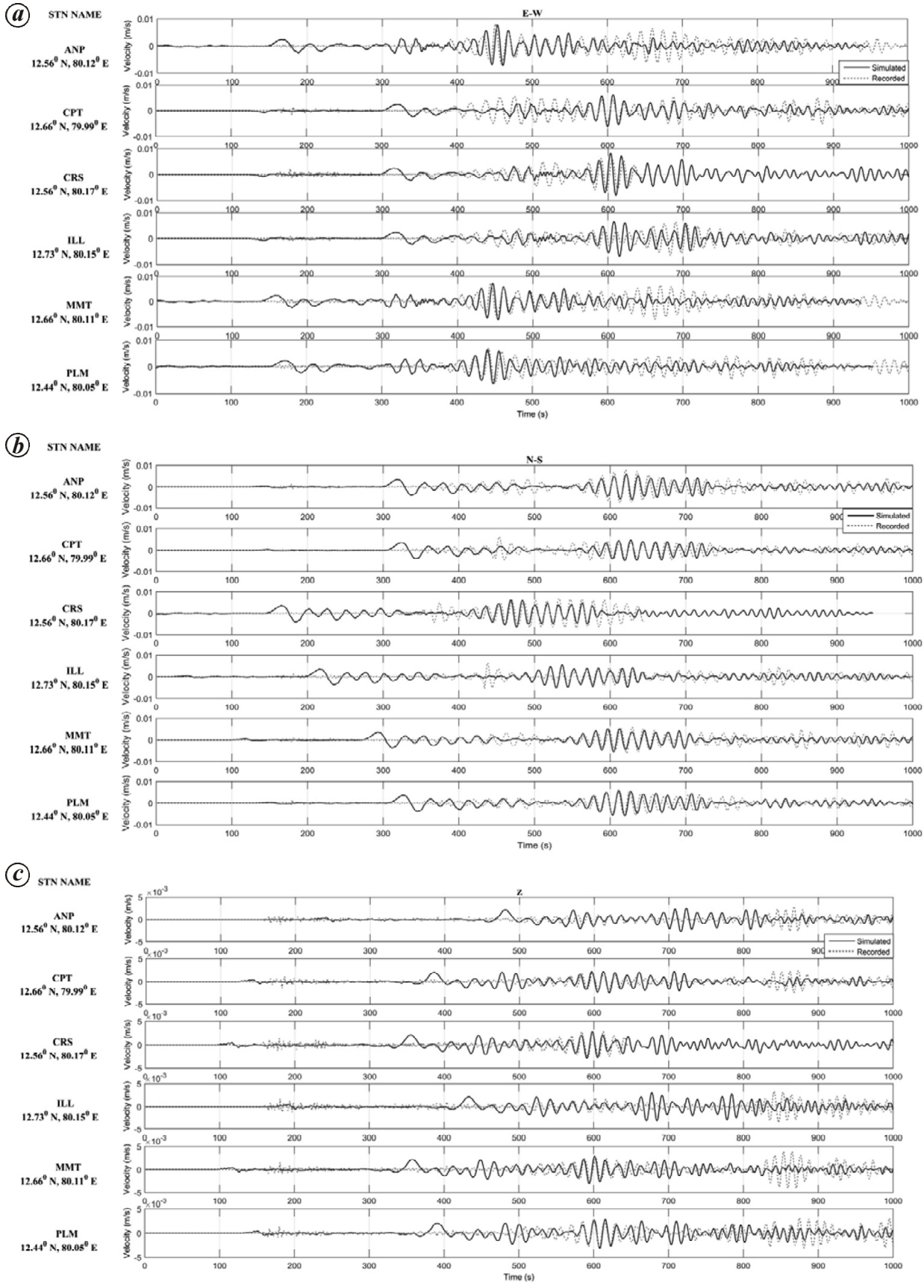

Figure 5. Comparison of simulated data with the recorded data of 2012 (M_w 8.6) Sumatra Earthquake.

Table 2. Details of slip distribution of 2004 (M_w 9.1) Sumatra earthquakes

Slip parameters	2004 Sumatra earthquake		
	Ammon *et al.*[3]	Ji[4]	Rhie *et al.*[5]
Longitude, latitude	95.78, 3.3	95.78, 3.3	95.49, 3.12
Depth (km)	35	35	27
Length (km)	1480	450	1355
Number of segments	3	1	6
Hypocenter			
Along strike (km)	70 in Seg. 1	52.5	43.91 in Seg. 1
Down-dip (km)	168 in Seg. 1	150	27 in Seg. 1
Segment			
Length (km)	300, 680, 500	450	350, 343, 162.50, 162.50, 165.50, 162.50
Width (km)	224, 192, 176	180	188.64, 144.88, 129.47, 129.47, 129.47, 129.47
Strike (°)	315, 342, 5	320	322, 343, 350, 0, 7, 24
Dip (°)	12, 15, 17.5	11	11, 15, 18, 18, 18, 18
Average rake (°)	99	91.7	100
Number of sub-faults	210, 408, 275	450	66, 55, 20, 20, 20, 20
Size of sub-faults (km)	20 × 16	15 × 12	31.82 × 31.44
Avg. rupture velocity (km/s)	3	2	2.5
Max. slip (m)	11.5	20	35

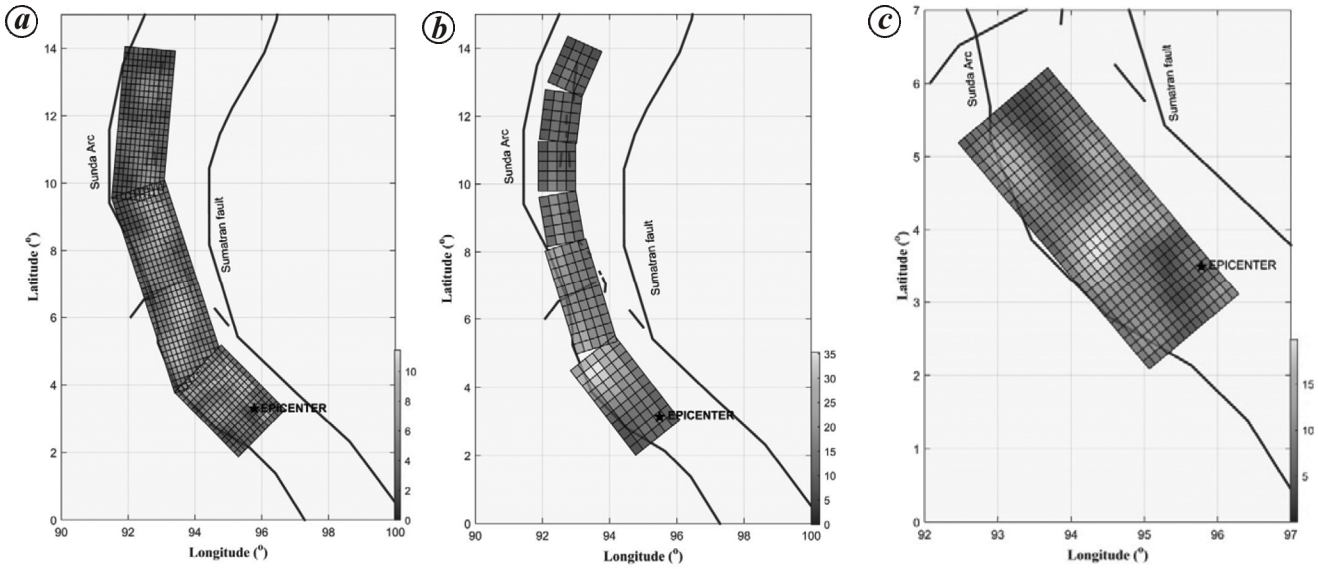

Figure 6. Slip distribution (in meter) for 2004 (M_w 9.1) Sumatra earthquakes: ***a***, Ammo *et al.*[3]; ***b***, Ji[4]; ***c***, Rhie *et al.*[5].

plain makes with respect to horizontal surface) of 64°. The ground motion simulated with this slip distribution as input at the six stations in the IGCAR network along with the recorded data is shown in Figure 5. It is noted that the *P* wave arrival and subsequent peaks of the simulated data match with the recorded data. The maximum amplitudes and phase for EW, NS and Z directions of simulated data also matched with recorded data. The slight variations between data might be due to the noise encountered in the instrument while recording the ground motions. The favourable comparison from the plot indicates that the SPECFEM model considered can be applied to get a realistic estimate of ground motion during an event in the region. Hence the same model with the source characteristics defined in the global database for 2004 Sumatra earthquake (M_w 9.1) is used to estimate the ground motion at various stations due to this event. The results obtained can also be used to get an estimate of the sensitivity of ground motion on different slip models for a great earthquake as explained further.

Source models for the 2004 Sumatra earthquake

The SPECFEM model is now employed to simulate ground motions for 2004 Sumatra earthquake. The three input slip models available in the global database for the

2004 Sumatra earthquake are summarized in Table 2 and is depicted in Figure 6. Ammon *et al.*[3] developed the slip distribution considering the teleseismic body waves (20–200 s), intermediate-period three-component regional seismograms (50–500 s) and long period teleseismic seismograms (250–2000 s). The rupture surface so obtained is in three segments (Figure 6 *a*). The hypocentre of this slip distribution lies in the first segment at a distance of 70 km along strike and 168 km along the dip direction respectively. The maximum slip is reported as 11.5 m. The second model considered in the present study is that reported by Ji[4] which was developed using 15 teleseismic *P* waveforms and 13 shear waveforms selected from GSN broadband data of IRIS-Data Management Center. This slip model (Figure 6 *b*), with epicentre at 3.30°N, 95.78°E and 35 km depth, has a single rupture plain of length of 450 km along strike angle of 320° and 180 km along dip angle of 11°. The fault plane is discretized into 450 subfaults of dimension 15 × 12 km, with maximum slip in measuring to be 20 m. The third model considered here is by Rhie *et al.*[5] obtained by using least-square inversion algorithm on data recorded in 10 IRIS and GEOSCOPE stations with an epicentral range of 43.6°–65.2°. An average rupture velocity of 2.5 km/s is considered. The slip is distributed into six segments with varying dip and strike angles as shown in Figure 6 *c* and summarized in Table 2. The maximum slip is reported as 35 m. The sensitivity of these slip models is analysed by simulating and comparing the ground motions at various stations as explained further.

Simulated ground displacements for 2004 Sumatra earthquake

The SPECFEM model in the present study is used to simulate ground time histories for a length of 30 min owing to the large rupture time of the slip models. These time histories simulated at various stations for the slip models considered for the study are shown in Figure 7. It is evident that the variation of ground motion for different slip models considered is more for the stations in near-field when compared to that at the far field. For the time histories of the near field stations represented in Figure 7 *a* the maximum amplitude varies from 0.25 to 1 m between different slip models. Considerable difference was observed in the ground motion pattern between the slip models in the near-field, though the arrival time is observed to be the same. The orders of permanent ground displacement at the stations are also observed to be differing with slip models. On the other hand, the amplitudes of displacement time histories are observed to be in the same order for the station in the far-field (Figure 7 *b*). But, the phase and arrival times varied with slip models for stations in the far-field. This highlights the influence of the slip model on both near and far field stations. The huge rupture length and the associated energy of the great earthquake considered in this study might be the reason for such a pattern.

The spatial variability of ground motion pattern near the epicentral region is demonstrated through contour maps in terms of PGD and GRD. For this purpose, the displacement field is calculated at a spacing of 6.6 km covering a region of dimension 660 × 1650 km around the fault (91°–97°E, 0°–15°N). The PGD and GRD contours for different slip models (Figures 8 and 9 respectively) indicate that the maximum displacement is observed near the region of maximum slip of each slip model. The distribution of the low-frequency ground displacement and the radiation pattern is observed to be in conjunction with the respective slip distribution. The PGD obtained from various slip models in horizontal and vertical direction vary between 14–22 m and 7–16 m respectively. From the GRD contours shown in Figure 9, it is clear that the ground is permanently displaced both vertically up and towards south west directions after the rupture process. The maximum permanent ground displacement ranges between 6–17, 4–17 and 2–8 m respectively for East–West, North–South and vertical direction between each slip distribution considered. This amplitude and the dynamic characteristic of the ground displacement on ocean bed displaces huge amount of water, which then results in triggering the tsunami wave propagation.

Summary and conclusion

The present study focuses on proposing a model to simulate ground motions for earthquakes in Sumatran region. The model is based on spectral finite element method. The model developed for the region is first validated with the recorded data available in IGCAR network for the 2012 (M_w 8.6) Sumatra earthquake. The favourable comparison of the model showed that it can be used to simulate reliable ground motions for the 2004 (M_w 9.1) Sumatra earthquake. The simulations for 2004 Sumatra earthquake are performed with three different slip distributions available in the global database. This highlights the sensitivity of ground motion to the slip distribution. Thus, for the near field stations, the variation is observed in the order of 0.75 m whereas for far-field stations the corresponding difference is negligible. Permanent ground displacement is also observed for stations in the near field. The spatial distribution of the ground displacement near the epicentral region in terms of PGD and GRD also emphasizes on the effect of the slip distribution on ground displacement. The variations with respect to slip models on the ground motion point to the uncertainty associated with source characterization. The model proposed in this study can be further used to simulate ground motions for various earthquakes in the region. The

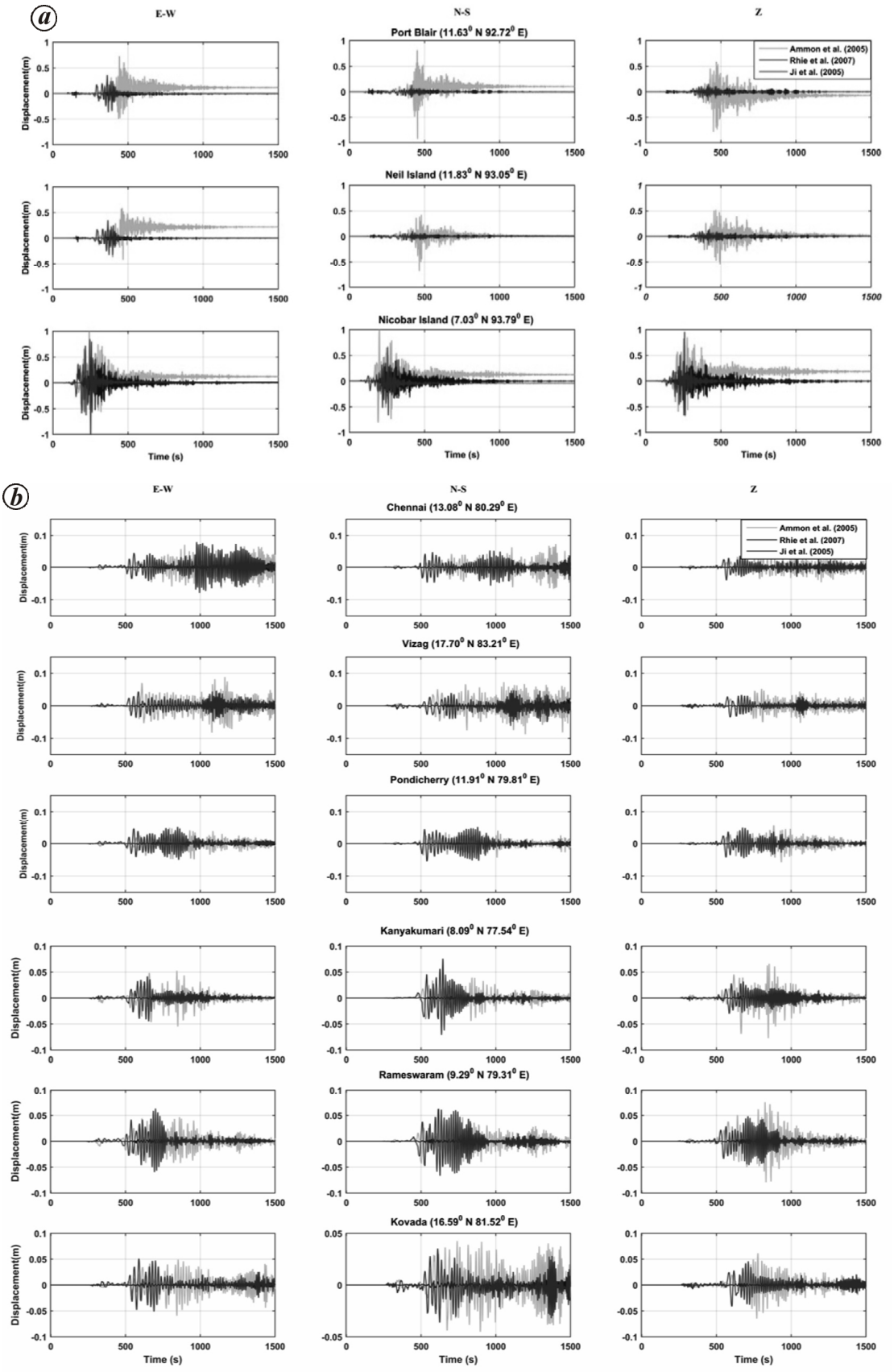

Figure 7. Displacement time history for 2004 (M_w 9.1) Sumatra earthquakes: ***a***, stations near the epicentral region (near- field); ***b***, stations far from the epicentral region (far-field).

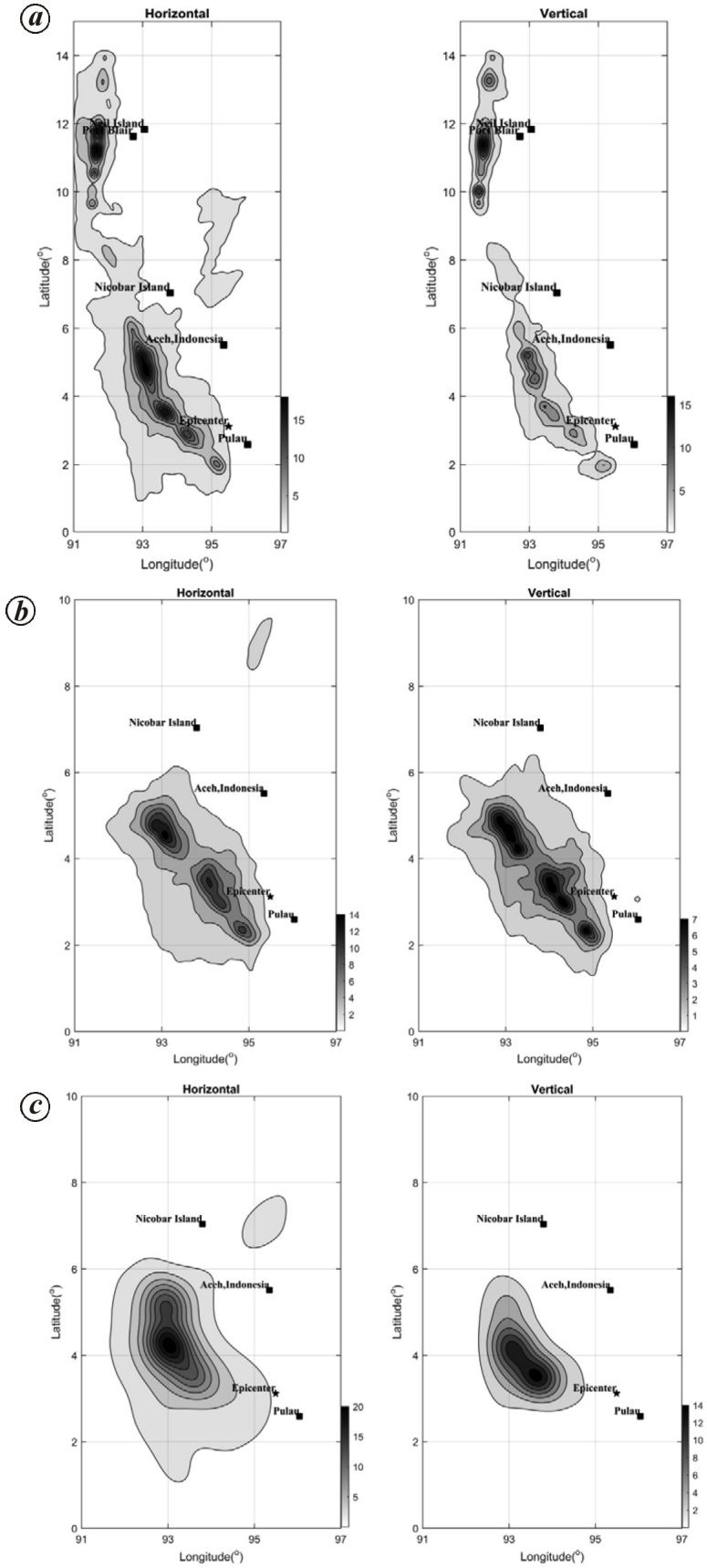

Figure 8. Peak ground displacement contours (in meter) for 2004 (M_w 9.1) Sumatra earthquake corresponding to different slip models: ***a***, Ammo *et al.*[3]; ***b***, Ji[4]; ***c***, Rhie *et al.*[5].

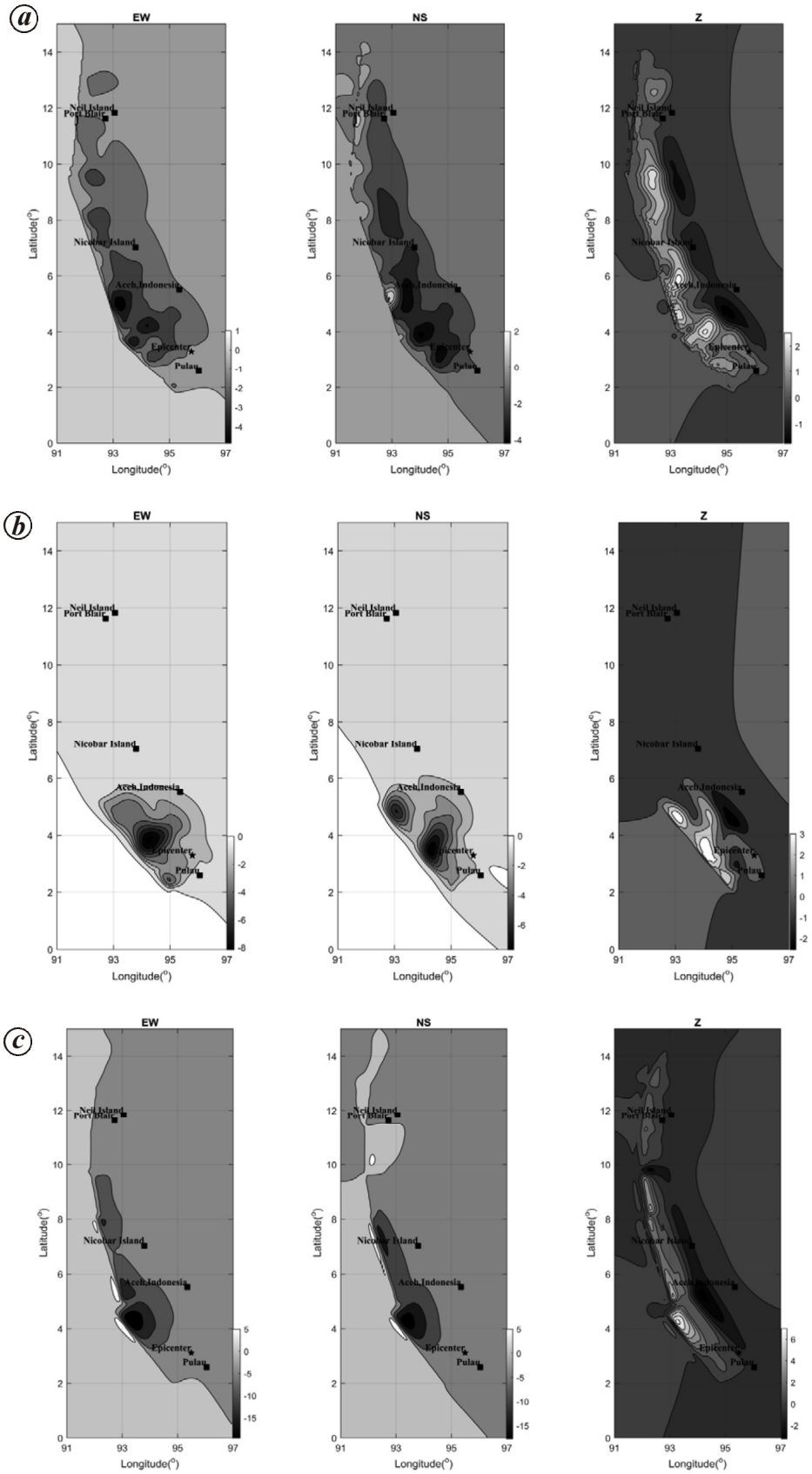

Figure 9. Ground residual displacement (in meter) contours for 2004 (M_w 9.1) Sumatra earthquake corresponding to different slip models: ***a***, Ammo *et al.*[3]; ***b***, Ji[4]; ***c***, Rhie *et al.*[5].

estimated ground motions can be used in various fields like the design of structures, estimation of tsunami generation potential and hazard analysis.

1. Pailoplee, S. and Choowong, M., Earthquake frequency-magnitude distribution and fractal dimension in mainland Southeast Asia. *Earth, Planets Space*, 2014, **66**(1), 1–10.
2. Ortiz, M. and Bilham, R., Source area and rupture parameters of the 31 December 1881 M_w = 7.9 Car Nicobar earthquake estimated from tsunamis recorded in the Bay of Bengal. *J. Geophys. Res. Solid Earth*, 2003, **108**(B4), 2215; doi:10.1029/2002JB001941
3. Ammon, C. J. *et al*., Rupture process of the 2004 Sumatra–Andaman earthquake. *Science*, 2005, **308**(5725), 1133–1139.
4. Ji, C., Preliminary rupture model for the December 26, 2004 earthquake, off the west coast of northern Sumatra, magnitude 9.1, 2005; http://neic.usgs.gov/neis/eq_depot/2004/eq_041226/neic_slav_ff.html
5. Rhie, J., Dreger, D., Bürgmann, R. and Romanowicz, B., Slip of the 2004 Sumatra–Andaman earthquake from joint inversion of long-period global seismic waveforms and GPS static offsets. *Bull. Seismol. Soc. Am.*, 2007, **97**(1A), S115–S127.
6. Titov, V., Rabinovich, A. B., Mofjeld, H. O., Thomson, R. E. and González, F. I., The global reach of the 26 December 2004 Sumatra tsunami. *Science*, 2005, **309**(5743), 2045–2048.
7. Murty, T. S., Nirupama, N., Nistor, I. and Hamdi, S., Far field characteristics of the tsunami of 26 December 2004. *ISETJ Earthq. Technol.*, 2005, **42**(4), 213–217.
8. George, D. L. and Randall, J. LeVeque, Finite volume methods and adaptive refinement for global tsunami propagation and local inundation. *Sci. Tsunami. Haz.*, 2006, **24**(5), 319–328.
9. Singh, A. P., Murty, T. S., Rastogi, B. K. and Yadav, R. B. S., Earthquake generated tsunami in the Indian Ocean and probable vulnerability assessment for the east coast of India. *Mar. Geodesy*, 2012, **35**(1), 49–65.
10. Roshan, A. D., Basu, P. C. and Jangid, R. S., Tsunami hazard assessment of Indian coast. *Nat. Hazards*, 2016, **82**(2), 733–762.
11. Sørensen, M. B., Atakan, K. and Pulido N., Simulated strong ground motions for the great *M* 9.3 Sumatra–Andaman earthquake of 26 December 2004. *Bull. Seismol. Soc. Am.*, 2007, **97**(1A), S139–S151.
12. LeVeque, R. J., George, D. L. and Berger, M. J., Tsunami modelling with adaptively refined finite volume methods. *Acta Numerica*, 2011, **20**, 211–289.
13. Okada, Y., Surface deformation due to shear and tensile faults in a half-space. *Bull. Seismol. Soc. Am.*, 1985, **75**(4), 1135–1154.
14. Ramadan, K. T., Hassan, H. S. and Hanna, S. N., Modeling of tsunami generation and propagation by a spreading curvilinear seismic faulting in linearized shallow-water wave theory. *Appl. Math. Model.*, 2011, **35**(1), 61–79.
15. Raghukanth, S. T. G. and Bhanu Teja, B., Ground motion simulation for 26 January 2001 Gujarat earthquake by spectral finite element method. *J. Earthq. Eng.*, 2012, **16**(2), 252–273.
16. Jayalakshmi, S. and Raghukanth, S. T. G., Regional ground motion simulation around Delhi due to future large earthquake. *Nat. Hazards*, 2016, **82**(3), 1479–1513.
17. Dhanya, J., Gade, M. and Raghuanth, S. T. G., Ground motion estimation during 25 April 2015 Nepal earthquake. *Acta Geod. Geophys.*, 2016; doi:10.1007/s40328-016-0170-8
18. Kayal, J. R., *Microearthquake Seismology and Seismotectonics of South Asia*, Capital Publishing Company, New Delhi, 2008.
19. IS: 1893, Criteria for earthquake resistant design of structures: Part 1 – General provisions and buildings, Bureau of Indian Standards (BIS), New Delhi, 2002.
20. Genrich, J. F., Bock, Y., McCaffrey, R., Prawirodirdjo, L., Stevens, C. W., Puntodewo, S. S. O., Subarya, C. and Wdowinski, S., Distribution of slip at the northern Sumatran fault system. *J. Geophys. Res.*, 2000, **105**(B12), 28–327.
21. Bock, Y. E. H. U. D. A., Prawirodirdjo, L., Genrich, J. F., Stevens, C. W., McCaffrey, R., Subarya, C., Puntodewo, S. S. O. and Calais, E., Crust al motion in Indonesia from global positioning system measurements. *J. Geophys. Res. Solid Earth*, 2003, **108**(B8).
22. Rajendran, C. P., Earnest, A., Rajendran, K., Das, R. D. and Kesavan, S., The 13 September 2002 North Andaman (Diglipur) earthquake: an analysis in the context of regional seismicity. *Curr. Sci.*, 2003, **84**(7), 919–924.
23. Bilham, R., Engdahl, R., Feldl, N. and Satyabala, S. P., Partial and complete rupture of the Indo-Andaman plate boundary 1847–2004. *Seismol. Res. Lett.*, 2005, **76**(3), 299–311.
24. Kavitha, B. and Raghukanth, S. T. G., Stochastic earthquake ground motion model for east coast region of India. *Life Cycle Reliability Safety Eng.*, 2013, **2**(3), 41–56.
25. Patera, A. T., A spectral element method for fluid dynamics: lamina r flow in a channel expansion, *J. Comput. Phys.*, 1984, **54**(3), 468–488.
26. Komatitsch, D. and Tromp, J., Introduction to the spectral element method for 3-D seismic wave propagation. *Geophys. J. Int.*, 1999, **139**(3), 806–822.
27. Komatitsch, D. and Tromp, J., Spectral-element simulations of global seismic wave propagation–I. validation. *Geophys. J. Int.*, 2002, **149**, 390–412.
28. Komatitsch, D. and Tromp, J., Spectral-element simulations of global seismic wave propagation–II. 3-D models, oceans, rotation, and self-gravitation. *Geophys. J. Int.*, 2002, **150**, 303–318.
29. Kustowski, B., Ekström, G. and Dziewoski, A. M., Anisotropińc-shear-wave velocity structure of the Earth's mantle: a global model. *J. Geophys. Res. Solid Earth*, 2008, **113**(B6).
30. Wei, S., April/11/2012 (M_w 8.6), Sumatra. Source Models of Large Earthquakes, Caltech, 2012; http://www.tectonics.caltech.edu/slip_history/2012_Sumatra/index.html (last accessed on 1 July 2013).
31. GSI, Seismotectonic Atlas of India and its Environs, Geological Survey of India, 2000.

ACKNOWLEDGEMENTS. We thank IGCAR for giving access to the ground motion records of 2012 Sumatra earthquake, which are used in validating the model developed in the present study.

Received 24 January 2017; revised accepted 22 November 2017

doi: 10.18520/cs/v114/i08/1709-1720